

# **Mildly Acidic Aluminosilicate Catalysts for Stable Performance in Ethanol Dehydration**

**Ales Styskalik,<sup>a,b,c</sup> Vit Vykoukal,<sup>c</sup> Luca Fusaro,<sup>d</sup> Carmela Aprile,<sup>d</sup> Damien P. Debecker<sup>\*a</sup>**

<sup>a</sup>Institute of Condensed Matter and Nanoscience (IMCN), UCLouvain, Place Louis Pasteur 1, 1348 Louvain-La-Neuve, Belgium

<sup>b</sup>Masaryk University, Department of Chemistry, Kotlarska 2, CZ-61137 Brno, Czech Republic

<sup>c</sup>Masaryk University, CEITEC MU, Kamenice 5, CZ-62500 Brno, Czech Republic

<sup>d</sup>Department of Chemistry, Unit of Nanomaterials Chemistry, University of Namur, 5000 Namur, Belgium

\*Corresponding author ([damien.debecker@uclouvain.be](mailto:damien.debecker@uclouvain.be)).

## ABSTRACT

Ethanol dehydration is effectively catalyzed by strongly acidic zeolite catalysts which are known, however, to exhibit poor time on stream stability. Alumina and silica-alumina on the other hand are relatively stable but reach only low activity levels. Here, a series of aluminosilicate catalysts (Si:Al ratio = 16) was prepared by non-hydrolytic sol-gel (NHSG) and are shown to feature an intermediate level of activity, between the HZSM-5 zeolite and a commercial silica-alumina. Importantly, the best samples, were very stable with time on stream. Unlike HZSM-5, which also catalyzes ethylene oligomerization due to its strong acid sites and is therefore prone to coking, NHSG prepared catalysts did not produce any traces of ethylene oligomers and did not show any trace of coke formation. Characterization (ICP-OES, N<sub>2</sub> physisorption, TEM, XPS, IR coupled with pyridine adsorption, Raman spectroscopy, solid state NMR spectroscopy) reveal that the unconventional synthetic method presented here allowed to prepare mesoporous aluminosilicate materials with a remarkable degree of homogeneity. It is this thorough dispersion of Al in the amorphous silicate matrix which is responsible for the formation of acid sites which are intermediate (in terms of strength and nature) between those of commercial silica-alumina and HZSM-5 zeolite. The texture of the best NHSG catalyst – mainly mesoporous with a high specific surface area (800 m<sup>2</sup> g<sup>-1</sup>) and pore volume (0.5 cm<sup>3</sup> g<sup>-1</sup>) – was also unaffected after reaction. To overcome deactivation issues in ethanol dehydration, this study suggests to target amorphous aluminosilicate catalysts with open mesoporosity and with an intimate mixing of Al and Si.

**Keywords:** mesoporous aluminosilicate; heterogeneous catalysis; non-hydrolytic sol-gel, ethanol dehydration; coke resistance

## 1. Introduction

The dehydration of bio-alcohols is an important catalytic reaction in the perspective of the development of a bio-based industry.[1,2] Bioethanol, for example, is a major bio-based platform chemical as its production via fermentation processes is now well-established. The total annual world ethanol production is above  $10^{11}$  liter and is expected to grow gradually.[3] Gas phase dehydration of bioethanol constitutes a relevant “drop-in” strategy, by which the produced bio-ethylene can be further exploited in the regular chemical processes that use ethylene (e.g. polyethylene manufacture).[4] Industrially, ethanol dehydration is carried out over solid acid catalysts with alumina and HZSM-5 zeolite being the most widely applied and thus used as benchmark catalysts.[2,5–9] Heteropolyacids and their salts,[10,11] amorphous silica-alumina,[12,13] transition metal oxides,[14] impregnated phosphoric acid,[15] and silicoaluminophosphates[16–18] can be named among other frequently studied catalysts.

Alumina is the traditional catalyst and is still industrially used in ethanol dehydration. It features a moderate activity, low degree of coking and therefore a relatively good stability with time on stream (TOS).[5] However it is necessary to apply fairly high temperatures (300–500 °C) in order to achieve reasonable ethylene productivities.[17,19] HZSM-5 zeolite is a highly active catalyst in ethanol dehydration. While it produces vast amounts of diethylether at low temperatures (i.e. in the 150–250 °C range), it is highly selective to ethylene at higher temperatures (i.e. 250–400 °C); ethylene yields higher than 98 % have been reported.[20] The well-known drawback of this catalyst, however, is its relatively fast deactivation due to coke formation: the strong Brønsted acid sites in HZSM-5 promote not only ethanol dehydration, but also ethylene oligomerization, consequently leading to the deposition of carbonaceous by-products on the catalyst surface.[16,17,21,22] This phenomenon impedes the industrial application of HZSM-5 in (bio)ethanol dehydration.

Many studies are therefore devoted to the modification of HZSM-5 zeolite in order to improve its coking resistance. Reported strategies comprise (i) decrease of strength and/or number of strong acid sites and (ii) mass transfer improvement. The former approach has been achieved by exchange of  $H^+$  for metal cations (e.g.  $Fe^{3+}$ ),[23] dealumination (e.g. by  $H_3PO_4$ ,[24]  $(COOH)_2$ ,[25]  $(NH_4)_2SiF_6$ ),[26] and by mitigation of surface acidity with water (i.e. working with mixed

ethanol/water feeds).[21,27] The latter approach has been achieved by the introduction of meso- and macropores into the microporous zeolite (e.g. by desilication with NaOH,[28] steam treatment,[29] etc.) or by decreasing the primary zeolite particles size from the micro- to the nano- range.[22,30]

Instead of using multistep and laborious procedures to tune down the acidity and disrupt the structure of the naturally microporous and strong solid acid HZSM-5, we suggest that other catalysts should be explored. Ideally, these materials should be mesoporous and possess high amounts of medium strength acid sites but a low amount of strong acid sites. Amorphous silica-alumina materials (ASA) have been envisaged as an alternative to HZSM-5 but they are usually not competitive due to low acidity and activity in comparison to zeolites. As an example industrial silica-alumina catalysts with a broad range of Si/Al molar ratios (5–87 wt% SiO<sub>2</sub>) were much less active than zeolites and had a comparable activity to plain alumina.[12,19,31]

Attempts to elucidate the working behavior of acidic aluminosilicate catalysts in ethanol dehydration have been carried out on model materials, e.g. aluminosilicates prepared by sol-gel and by grafting of SiO<sub>2</sub> on top of Al<sub>2</sub>O<sub>3</sub> and vice versa.[32–36] Studies on these model materials helped understand that classical amorphous silica alumina should be considered as mixtures of silica and alumina domains, and that mostly the latter domains govern the catalytic behavior. These results may explain the low activity of industrial ASAs and suggest that an improvement in catalytic activity can be achieved with better homogeneity of Al-Si dispersion. Indeed model catalysts made by sol-gel, which featured higher homogeneity,[33] displayed different acidic properties (i.e. stronger Brønsted acid sites). Recently, macro-mesocellular aluminosilicate foams were obtained using an unconventional synthetic technique based on sol-gel chemistry. The aluminum atoms were well incorporated within the silica network, the catalysts possessed more and stronger acid sites, and the ethylene productivity was more than 25 % higher in comparison to commercial silica-alumina.[37] However, it is noteworthy that the reports on ASAs in ethanol dehydration referred above focused on the catalytic activity, ethylene selectivity, and acid sites strength and number,[12,32,33,35,37] but did not describe the catalyst stability and propensity to coke formation.

Non-hydrolytic sol-gel (NHS) is a technique that allows attaining high level of homogeneity and excellent textural properties in mixed metal oxides.[38,39] It has been already used for the preparation of various types of porous mixed oxide catalysts including aluminosilicates with low Si/Al ratios[40,41], but also Ta promoted silica,[42] Co doped aluminosilicates,[43]  $\text{MoO}_3\text{-SiO}_2\text{-Al}_2\text{O}_3$ [44],  $\text{Re}_2\text{O}_7\text{-SiO}_2\text{-Al}_2\text{O}_3$ [45], and other metallosilicates and metalloaluminates (M = Ti, Zr, W, etc.).[38,39] The versatility of this preparation route prompted us to explore the potential of NHS-prepared amorphous aluminosilicate in the dehydration of ethanol. Our hypothesis was that the high homogeneity of Si-Al dispersion (intrinsic for NHS prepared materials)[38,39,46] should provide materials with an increased number of stronger acid sites. This fact can be reflected in higher catalytic activity in ethanol dehydration. Ideally, these acid sites should display lower strength than HZSM-5 and thus avoid coke formation.

Herein we present a one-step synthesis of highly homogeneous amorphous aluminosilicates with medium strength acid sites. The texture and homogeneity of these porous catalysts were controlled by tuning the NHS reaction conditions. Their performance are tested in the dehydration of ethanol and compared to HZSM-5 and commercial silica-alumina as benchmarks. Their remarkable performance – in particular in terms of stability against coking – are interpreted using an array of physico-chemical characterization tools.

## 2. Experimental

**General experimental methods, characterizational techniques, and spectroscopic characterization data** (IR and NMR) can be found in the supporting material to this manuscript (ESI).

**2.1 Xerogel synthesis – acetamide elimination route.** 6.7243 g (25.45 mmol) silicon tetraacetate was loaded in an autoclave in a glove box and dissolved in 40 cm<sup>3</sup>  $\text{CH}_2\text{Cl}_2$ . In a separate vial, 0.2591 g (1.627 mmol)  $\text{Al}(\text{NMe}_2)_3$  was dissolved in  $\text{CH}_2\text{Cl}_2$  (5 cm<sup>3</sup>) and stirred at RT for 5 min. The solution of  $\text{Al}(\text{NMe}_2)_3$  was then added to the solution of silicon tetraacetate under vigorous stirring (5 min). The autoclave was sealed and kept in an oven at 160 °C for 72 h. During this time, gelation occurred. After cooling down, the autoclave was put back into the glovebox, opened and the gel was transferred into a Schlenk vessel. The gel was then dried under vacuum at 60 °C overnight in

order to remove the solvent and volatile condensation products (N, N'-dimethylacetamide and acetic acid anhydride). The resulting powder was calcined in flowing air at 500 °C (5 °C min<sup>-1</sup>, 5 h) yielding a pale yellow catalyst (**16Si-1Al-Ac**), where 16 is the molar ratio between the silicon precursor and the aluminum precursor (nominal molar Si/Al ratio = 16) and “Ac” stands for “acetamide elimination route”. Textural properties were varied by the addition of a surfactant into the solution of silicon tetraacetate before aluminum precursor addition (2.2929 g of Pluronic F127, sample **16Si-1Al-Ac-T**, where T stands for “templated”).

Table 1: Synthesis, XPS, and ICP-OES data for NHSG-made aluminosilicate catalysts.

Sample	n <sub>Si</sub> <sup>a</sup> (mmol)	n <sub>Al</sub> <sup>b</sup> (mmol)	n <sub>DIPE</sub> <sup>c</sup> (mmol)	Note	Si/Al ratio (-) Theor/ICP
16Si-1Al-Ac	25.52	1.582	-	-	16.1/17.2
16Si-1Al-Ac-T	25.45	1.627	-	2.2929 g F127 <sup>d</sup>	15.6/17.8
16Si-1Al-Et	28.63	1.821	59.90	-	15.7/17.5
16Si-1Al-Et-S	28.61	1.759	59.93	No solvent	16.3/16.3

<sup>a</sup>Si precursor = Si(OAc)<sub>4</sub> for acetamide elimination and SiCl<sub>4</sub> for alkylhalide elimination; <sup>b</sup>Al precursor = Al(NMe<sub>2</sub>)<sub>3</sub> for acetamide elimination and AlCl<sub>3</sub> for alkylhalide elimination; <sup>c</sup>DIPE = diisopropylether; <sup>d</sup>F127 = surfactant Pluronic F127.

**2.2 Xerogel synthesis – alkylhalide elimination (ether) route.** 6.1207 g (59.90 mmol) diisopropylether (DIPE) was loaded in an autoclave in a glove box and mixed with 45 cm<sup>3</sup> CH<sub>2</sub>Cl<sub>2</sub> and 4.863 g (28.63 mmol) silicon tetrachloride. 0.2428 g (1.821 mmol) AlCl<sub>3</sub> was added directly to the solution of silicon tetrachloride and diisopropylether under vigorous stirring (5 min). The autoclave was sealed and kept in an oven at 110 °C for 72 h. During this time, gelation occurred. After cooling down, the autoclave was put back into the glovebox, opened and the gel was transferred into a Schlenk vessel. The gel was then dried under vacuum at 60 °C overnight in order to remove the solvent and volatile condensation product (isopropylchloride). The resulting powder was calcined in a flow of air at 500 °C (5 °C min<sup>-1</sup>, 5 h) yielding a pale yellow catalyst (**16Si-**

**1Al-Et**), where “Et” stands for “ether route”. Textural properties were varied by avoiding the use of solvent (sample **16Si-1Al-Et-S**, where S stands for “solventless”).

**2.3 Ethanol dehydration.** The calcined xerogel catalysts (0.192 g, sieved in the 0.20–0.40 mm particle size range) were diluted with glass beads (0.5–1 mm) in order to keep the volume of the catalyst bed constant. The void space of the reactor was filled with silica beads. Catalytic testing was carried out by injecting 0.212 g h<sup>-1</sup> of absolute ethanol by means of NE-300 syringe pump in a 40 cm<sup>3</sup> min<sup>-1</sup> flow of N<sub>2</sub> (4.4 mol% of ethanol in N<sub>2</sub>). The tests were carried out at atmospheric pressure, WHSV = 1.1 h<sup>-1</sup>. Temperature was either maintained at a fixed temperature for 15 h or varied stepwise in the range from 205 to 310 °C by steps of 35 °C. One step consisted of (i) heating ramp (5 °C min<sup>-1</sup>) and stabilization at the set temperature (21 min) and (ii) steady temperature state (56 min). The analysis of the effluent gas was carried out by a VARIAN 3800 Gas Chromatograph (8 injections at each temperature) equipped with a flame ionization detector (FID) and a Cydex B column (25 m long, internal diameter 0.22 mm, film thickness 0.25 μm).

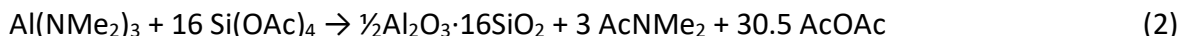
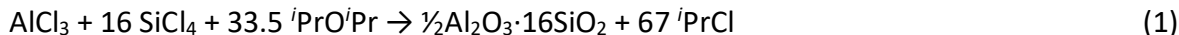
Stability tests were performed on fresh catalysts by maintaining a stable temperature (240 or 275 °C) for 15 h in order to study the effect of time on stream (TOS) on catalytic activity and selectivity. Maximum productivity was found by varying WSHV while keeping ethanol concentration in the feed constant. In case of HZSM-5 it was necessary to decrease the catalyst mass due to the high activity of this catalyst.

### **3. Results and discussion**

#### *3.1 Synthesis and characterization*

Aluminosilicate samples were prepared by NHSG, a technique which is known to produce mixed metal oxides with high homogeneity of metal mixing and good textural properties. [38,39,47] Two routes were applied – alkylhalide elimination (also called “ether route”, Eqn. 1) and acetamide elimination (Eqn. 2). Both of them are known to yield materials with a high homogeneity of metal mixing, but they show a significant difference in textural properties. While the former usually produces mesoporous materials with high pore volumes and its porosity is governed by reaction conditions (temperature, amount of solvent used, etc.), [44,48] the latter tends to produce

microporous samples and therefore its textural properties must often be improved by the addition of templating agents or by the application of organosilica precursors.[40,49–51]



Four samples were prepared – two by the ether route (with and without solvent) and two by the acetamide elimination route (with and without templating agent) in order to obtain a series of samples with different textural properties. These catalysts were denoted as **16Si-1Al-Et**, **16Si-1Al-Et-S**, **16Si-1Al-Ac**, and **16Si-1Al-Ac-T**. The nominal Si:Al ratio was chosen to be the same as in the benchmark catalyst HZSM-5 and kept constant for all four samples (Si:Al = 16). ICP-OES analysis confirmed, that NHSG provides samples with Si:Al ratios close to the nominal values (Table 1).

N<sub>2</sub> adsorption-desorption isotherms are shown in Fig. 1 and the corresponding data are summarized in Table 2. The difference between the two routes is clearly visible. The ether route produces samples with lower S<sub>BET</sub>, however the pore volumes are high (0.74 and 0.96 cm<sup>3</sup> g<sup>-1</sup> for the sample prepared with and without solvent, respectively). This is reflected in high average pore size (ca. 10 nm). The fact that the steep hysteresis loop is located at high partial pressures (0.8–1.0 p/p<sub>0</sub>) suggests that a significant fraction of the porosity originates from interparticle voids.[52] This is especially true for the sample **16Si-1Al-Et**, which displayed a non-uniform and very broad distribution of pore sizes (5 – 200 nm) according to BJH analysis (Fig. 1S). The sample prepared without any solvent (**16Si-1Al-Et-S**) is more uniform; it showed even distribution of the pores from 5 to 40 nm with a maximum around 10 nm (Fig. 1S). On the contrary, the sample prepared by acetamide elimination without template addition (**16Si-1Al-Ac**) only displays a strong adsorption at very low pressures (below 0.1 p/p<sub>0</sub>) meaning that it is fully microporous. This conclusion was supported by t-plot analysis, which indicated that 100 % of the total pore volume is formed by micropores (Table 2). Finally, a large fraction of mesopores (59 % of total pore volume) was introduced into the sample upon template addition (**16Si-1Al-Ac-T**). This strategy did not lead to the formation of well-calibrated mesopores such as those often reported in the



synthesis of materials by hydrolytic sol-gel chemistry using Pluronic F127 [53] (possibly because the apolar medium in NHSG affects the formation of surfactant micelles). Yet the introduction of the surfactant led to a significant increase in  $SA_{BET}$  and total pore volume (Table 2). These features were reflected in the BJH analysis of pore size distribution of the mesoporous sample (Fig. 1S).

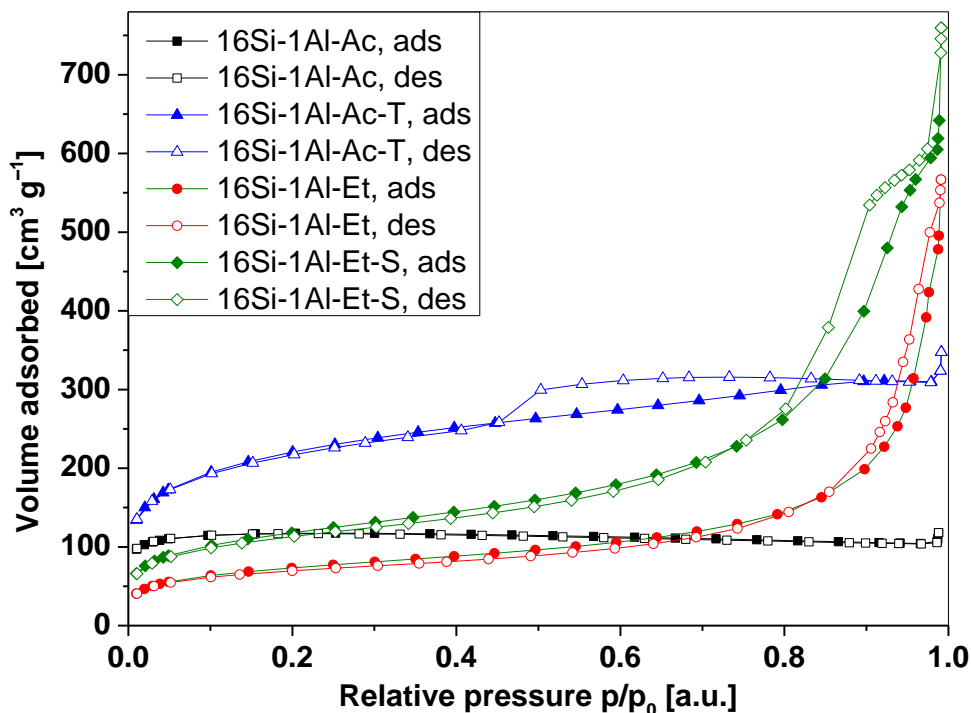


Fig. 1:  $N_2$  adsorption-desorption isotherms of NHSG-prepared samples.

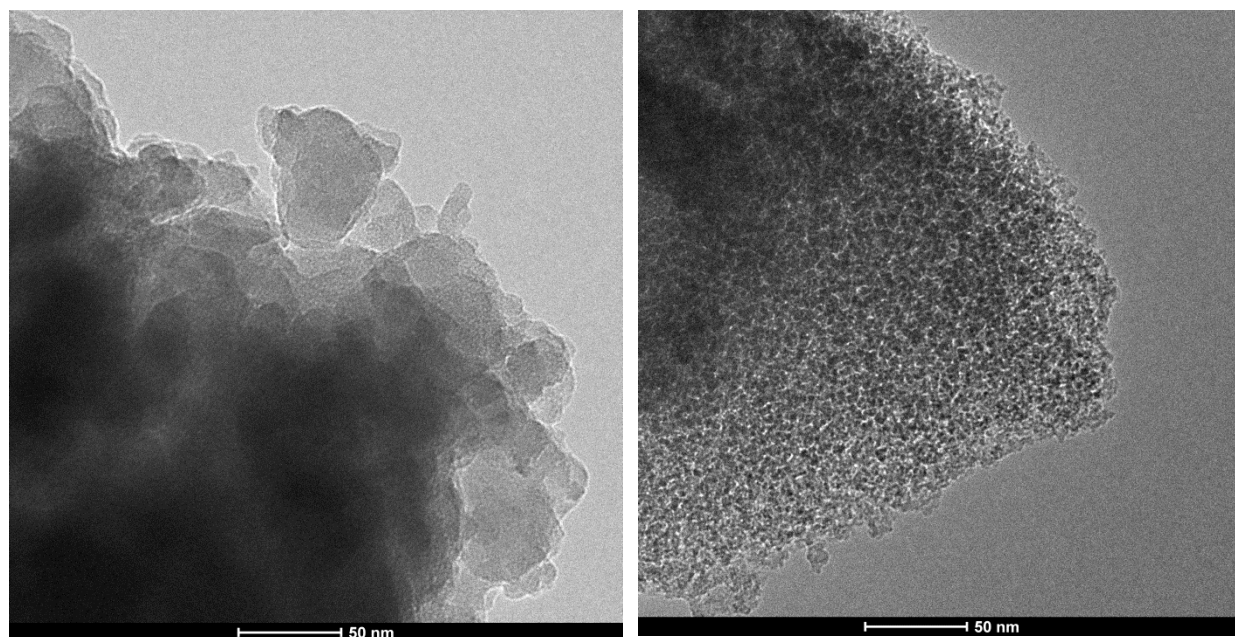
Table 2: Textural properties

Sample	Fresh catalyst				Spent catalyst <sup>a</sup>			
	$SA_{BET}$ ( $m^2 g^{-1}$ )	$V_{total}$ ( $cm^3 g^{-1}$ )	$D^b$ (nm)	$V_{micro}^c$ (%)	$SA_{BET}$ ( $m^2 g^{-1}$ )	$V_{total}$ ( $cm^3 g^{-1}$ )	$D^b$ (nm)	$V_{micro}^c$ (%)
16Si-1Al-Ac	470	0.17	1.4	100	270	0.078	1.2	100
16Si-1Al-Ac-T	800	0.50	2.5	41	740	0.50	2.7	41
16Si-1Al-Et	280	0.74	11	1	140	0.40	12	0

16Si-1Al-Et-S	420	0.96	9.1	5	290	0.46	6.3	6
---------------	-----	------	-----	---	-----	------	-----	---

<sup>a</sup>After 15 h on stream at 240 °C; <sup>b</sup> $4V_{\text{total}}/SA_{\text{BET}}$ ; <sup>c</sup>based on t-plot analysis.

The results of N<sub>2</sub> adsorption-desorption experiments were further corroborated by TEM. Micrographs show relatively big primary particles (in the range of tens and hundreds of nm) for **16Si-1Al-Ac** and **16Si-1Al-Ac-T** (Fig. 2S). A closer look at these particles reveals uniform intensity in TEM image of **16Si-1Al-Ac** (Fig. 2 top-left). The reason is that the micropores are too small to be observed with the magnification used. On the contrary, sample **16Si-1Al-Ac-T** (Fig. 2 top-right) displays mesopores within its structure originating from the presence of templating agent during polycondensation. The presence of the sacrificial template leads to the formation of “wormhole” motifs without long-range ordering, as observed in other NHSG syntheses applying templates.[52,54] In contrast to the samples synthesized by acetamide elimination, the TEM micrographs of **16Si-1Al-Et** (Fig. 2, down-left) and **16Si-1Al-Et-S** (Fig. 2, down-right) show agglomerates of smaller particles (ca. 10 nm). The intra-aggregate (i.e. inter-particle) voids form a relevant part of porosity as already suggested based on N<sub>2</sub> physisorption data.



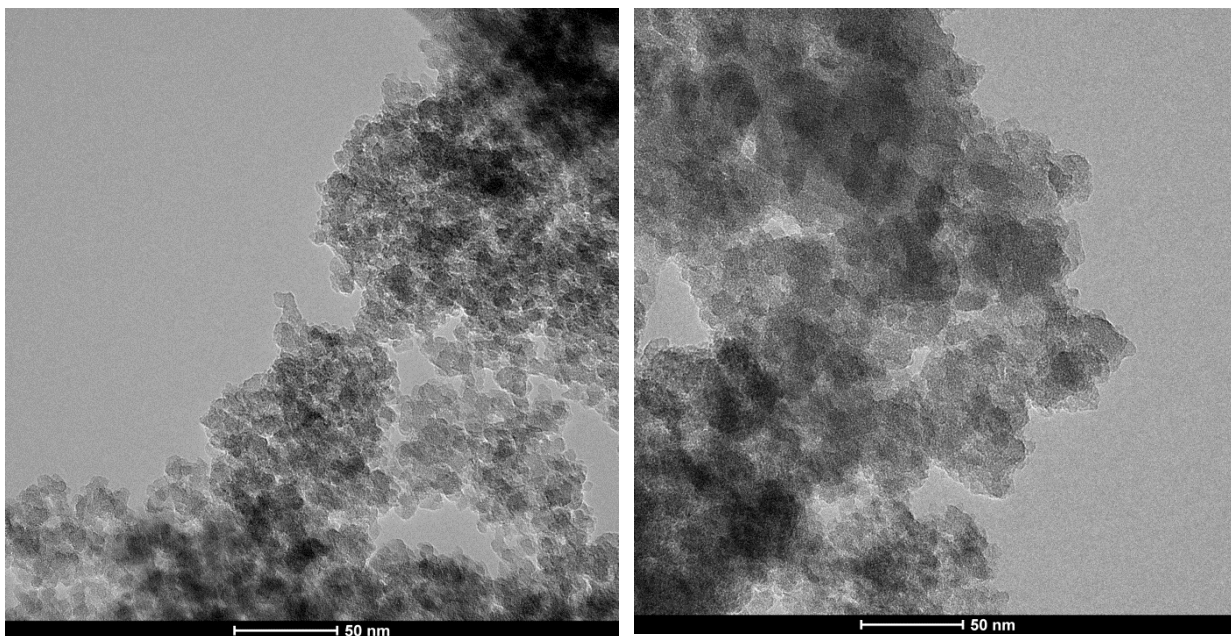


**Fig. 2:** TEM micrographs of aluminosilicate catalysts prepared by NHSG technique. Sample 16Si-1Al-Ac-T (top); sample 16Si-1Al-Et-S (down).

IR spectra were very similar for all four samples (Fig. 3S). The most intense absorption band at  $1076\text{--}1095\text{ cm}^{-1}$  was ascribed to the asymmetric valence vibration of Si–O–Si bridges. The redshift for this band in comparison to pure silica ( $1200\text{ cm}^{-1}$ ) is explained in the literature by the presence of Si–O–Al bridges.[55–57] Other absorption bands of lower intensity were observed at  $518\text{--}520$ ,  $798\text{--}810$ , and  $945\text{--}960\text{ cm}^{-1}$  and were assigned to Si–O–Si deformation vibration, symmetric Si–O–Si valence vibration, and Si–O–H deformation vibration, respectively. All observed absorption bands were thus attributed to typical vibration modes found in aluminosilicate matrices.

$^{29}\text{Si}$  CPMAS NMR spectra were also very similar for all four catalysts prepared by NHSG. The main signal was observed at  $-101\text{ ppm}$  with two shoulders of lower intensity at  $-91$  and  $-112\text{ ppm}$  (Fig. 4S). These signals were ascribed to  $\text{Si}(\text{OSi})_3(\text{OH/OAl})$ ,  $\text{Si}(\text{OSi})_2(\text{OH/OAl})_2$ , and  $\text{Si}(\text{OSi})_4$ , respectively.[58]

$^{27}\text{Al}$  MAS NMR spectra of samples exposed to ambient atmosphere (Fig. 3) showed always the most intense peak for  $\text{AlO}_4$  species at  $50\text{--}54\text{ ppm}$  confirming a good incorporation of aluminum into the silicate matrices in tetrahedral coordination.[58] Octahedrally coordinated Al atoms were

also observed (signal at 0 ppm) in NHSG prepared catalysts. Similar to extra-framework Al species in zeolites, these moieties can exist in different forms ranging from isolated and hydrated aluminum atoms not totally embedded in silica matrix to small alumina domains.[59,60] Finally all NHSG-prepared samples exhibited low amounts of  $\text{AlO}_5$  species based on the presence of a shoulder at ca. 25 ppm. The most relevant fraction of these moieties was observed in the case of sample **16Si-1Al-Ac**. It was reported recently that pentacoordinated Al atoms can exhibit Brønsted acidity and an exceptional activity in acid catalyzed reactions.[61–63] It is noteworthy that the  $^{27}\text{Al}$  MAS NMR spectra reported herein closely resembled “pre-zeolitic” amorphous aluminosilicates prepared by spray-drying procedure.[64]

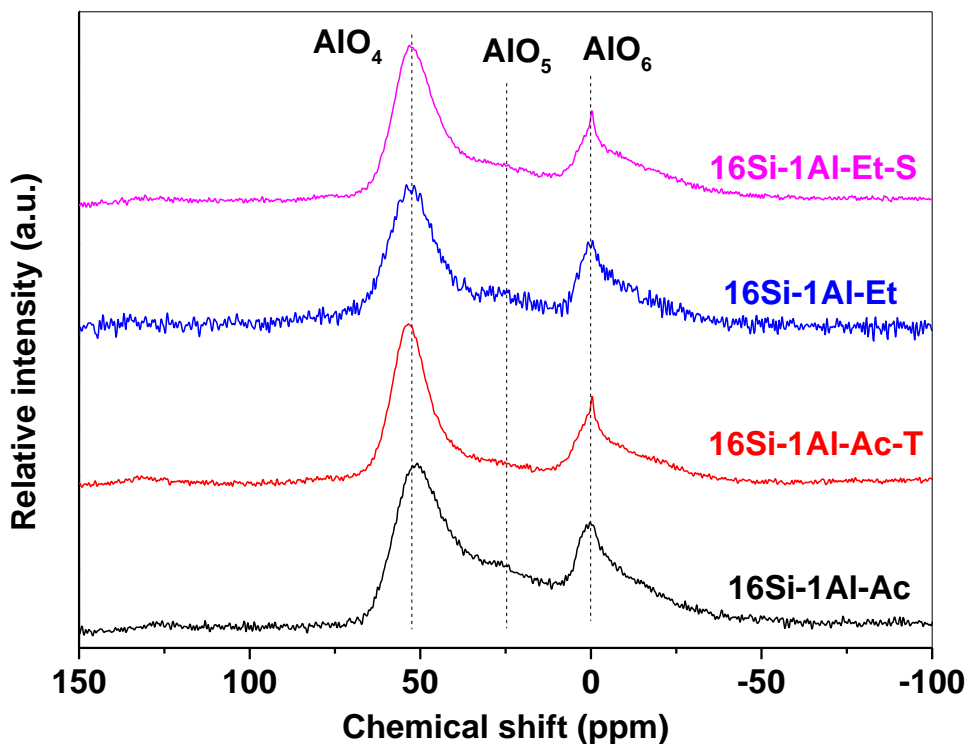


Fig. 3:  $^{27}\text{Al}$  MAS NMR spectra of NHSG prepared aluminosilicate catalysts.

Additional  $^{27}\text{Al}$  MAS NMR experiments were performed in order to gain a better description of  $\text{AlO}_6$  moieties present in NHSG prepared samples. When fully dehydrated, the aluminosilicate catalysts gave spectra with very broad signals coinciding with baseline; their assignment was not possible (Fig. 5S). Interestingly, the coordination of water molecules was fully and rapidly

reversible; degassed aluminosilicate catalyst exposed to ambient atmosphere for 10 min exhibited  $^{27}\text{Al}$  MAS NMR spectrum identical to the one before evacuation. This behavior has been already observed and is due to the presence of asymmetric (possibly tricoordinated) Al species.[60,65] Pyridine was adsorbed on dehydrated samples as a bulkier base in comparison to water and then the aluminosilicate catalysts were re-analyzed by  $^{27}\text{Al}$  MAS NMR spectroscopy (Fig. 4). This procedure led to a marked improvement in spectra quality. Strikingly, the only observed signal originated from tetrahedrally coordinated Al atoms. The fact that the signal of octahedrally coordinated Al atoms disappears upon dehydration and pyridine adsorption can be associated with the presence of isolated surface aluminum species (which are six-coordinated when hydrated but four-coordinated when in interaction with pyridine).[60,65] On the contrary, the possible presence of Al oxide oligomers or particles could be discarded since these  $\text{AlO}_6$  species would still be detected at  $\sim 0$  ppm upon dehydration and pyridine adsorption. These results point at the high homogeneity of NHSG prepared aluminosilicate catalysts.

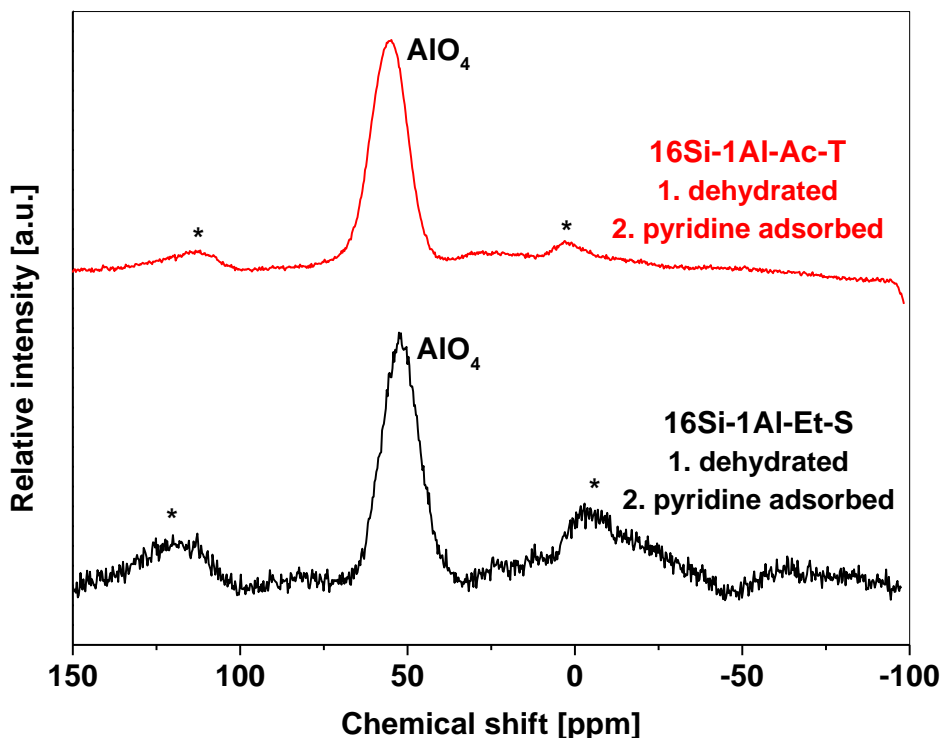


Fig. 4:  $^{27}\text{Al}$  MAS NMR spectra of NHSG prepared aluminosilicate catalysts after dehydration and pyridine adsorption, asterisks denote spinning sidebands.

The same procedure (dehydration followed by pyridine adsorption) was performed on the commercial silica alumina (SACS, Fig. 6S)[66]. While spectrum of hydrated sample was similar to NHSG prepared samples (mainly  $\text{AlO}_4$  and some  $\text{AlO}_6$  species), the spectrum after dehydration and pyridine adsorption revealed important differences. The intensities of signals originating in tetrahedrally and octahedrally coordinated Al atoms remained virtually the same thus pointing at the presence of alumina oligomers or particles in the commercial sample. This finding is in striking contrast to NHSG catalysts where the formation of alumina clusters was excluded.

The amount and nature of acid sites were determined by pyridine adsorption combined with IR spectroscopy (Table 3).[67] The total amount of Brønsted and Lewis acid sites was determined by integrating intensities of absorption band at 1545 and 1455  $\text{cm}^{-1}$ , respectively; molar extinction coefficients according to Emeis[67] were used in calculations. The strength of the acid sites was approached by looking at the fraction of sites that were preserved after degassing at 350°C. All four NHSG prepared samples were very similar – total amount of acid sites was similar, all of them displayed absorption bands due to both Brønsted and Lewis acid sites, and most of the Brønsted acid sites had lower strength than Lewis acid sites (Table 3, Fig. 5, Fig. 7S–9S). Finally the OH region in IR spectra (Fig. 10S) of all NHSG prepared samples displayed a narrow band at 3743  $\text{cm}^{-1}$ , characteristic for isolated hydroxyl groups on silica surfaces. Additionally, a broad band was detected at ca. 3680  $\text{cm}^{-1}$ , indicative of the presence of somewhat stronger Brønsted acid sites similar to other studies on aluminosilicates.[68–70]

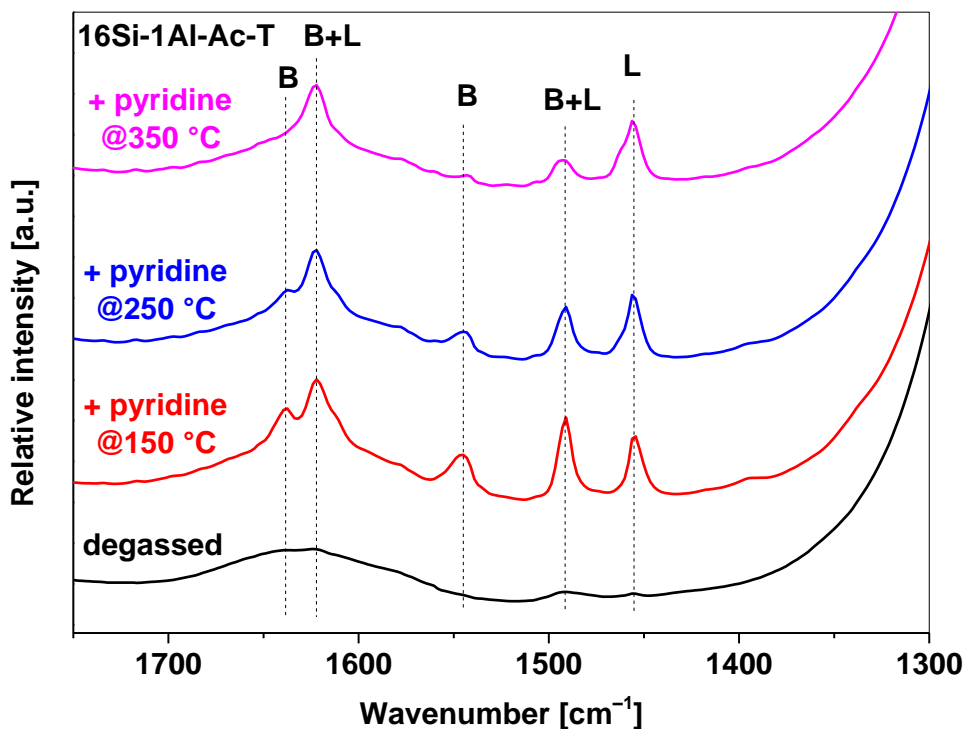


Fig. 5: IR spectra of 16Si-1Al-Ac-T, degassed, and after pyridine adsorption and degassed at different temperatures. Similar plots are provided in the ESI for the other NHSG samples (Fig. 7S-9S) and a quantitative analysis of the data is presented in Table 3.

The total amount of acid sites in NHSG prepared catalysts ranged from 0.042 to 0.064 mmol g<sup>-1</sup> (Table 3). These numbers are much lower than for both benchmark catalysts (0.22 mmol g<sup>-1</sup> and 0.14 mmol g<sup>-1</sup> for HZSM-5 and SACS, respectively, Fig. 11S and 12S). The higher amount of acid sites in the case of HZSM-5 comes from its uniform crystalline structure where each Al atom substituting Si in the matrix gives rise to a formal negative charge, which is compensated by an acidic proton associated with a Si–O–Al bridge.[71] SACS displays higher number of acid sites due to higher Al concentration.

**Table 3:** Amount, strength, and nature of acid sites in NHSG prepared aluminosilicates and commercial benchmark catalysts by pyridine adsorption combined with IR spectroscopy (spectra used to obtain this table are presented in Fig 4 and in ESI Fig. 7S-9S and Fig. 11S-12S).

Sample	Total acid sites (mmol g <sup>-1</sup> )	B/L ratio (-)	Acid sites after desorption at 350 °C (%)	B/L ratio after desorption at 350 °C

				(-)
16Si-1Al-Ac	0.064	0.47	79	0.16
16Si-1Al-Ac-T	0.054	1.1	59	0.25
16Si-1Al-Et	0.042	0.72	65	0.13
16Si-1Al-Et-S	0.046	0.83	65	0.21
HZSM-5	0.22	4.3	85	3.9
SACS	0.14	0.24	33	0.05

The nature of the acid sites also seems to follow an expected trend. On the one hand HZSM-5 is mostly governed by Brønsted acid sites (B/L ratio = 4.3) due to the reasons discussed above and well described in the literature.[71] On the other hand SACS shows mostly Lewis acid sites similar to  $\gamma$ -Al<sub>2</sub>O<sub>3</sub> (B/L ratio = 0.24).[32] This feature is due to a poor homogeneity of Si-Al mixing resulting in the occurrence of silica and alumina domains.[32,69] Finally samples prepared by NHSG are intermediate between these two extremes with B/L ratio ranging from 0.47 to 1.1.

The acid strength of NHSG samples seems to be intermediate between HZSM-5 and SACS as well. NHSG catalysts keep from 59 to 79 % of the total acid sites upon evacuation at 350 °C. Most of the lost acid sites are Brønsted in nature; B/L ratio decreases to values below 0.25. HZSM-5 displays high strength of acid sites; 85 % are retained upon degassing at 350°C, with only little change in the B/L ratio. Finally SACS maintains only 33 % of total acid sites pointing at their mostly weak character. The Brønsted acid sites almost completely disappeared upon evacuation at 350 °C; B/L reaches 0.05 only.

Analysis by pyridine adsorption combined with IR spectroscopy shows that NHSG prepared catalysts possess mainly Brønsted acid sites of medium strength (pyridine mostly desorbed at 350 °C) and strong Lewis acid sites (pyridine mostly retained after evacuation at 350 °C). Very low amount of strong Brønsted acid sites is observed as well. These general trends are similar to findings observed by Hensen et al. in amorphous aluminosilicates prepared by cogelation of sodium silicate with aluminum chloride and homogeneous deposition of alumina on silica



surface.[69,70] While the precise description of the acid sites in amorphous aluminosilicates is beyond the scope of this work, it can be put forward that the two mostly represented types of acid sites (medium Brønsted and strong Lewis) come from pseudobridging Si–OH...Al sites and isolated uncoordinated Al atoms, respectively.[69,72] It is noteworthy that the origin of acid sites in NHSG prepared catalysts (amorphous aluminosilicates with a good homogeneity of Si-Al mixing) is different than in the case of both benchmark catalysts (HZSM-5 with strong Brønsted acid sites typical for zeolites[71] and SACS with weak Lewis acid sites mostly originating from alumina domains[32,69]).

In summary, highly porous aluminosilicates were prepared by two NHSG routes. The porosity was controlled by the reaction conditions and ranged from micro to meso/(macro)porosity. In contrary to commercial silica-alumina, the aluminum atoms were well incorporated and homogeneously dispersed within the silica matrices. This in turn led to intermediate acidity of NHSG prepared samples – they exhibited stronger acid sites and higher B/L ratio than SACS, but weaker acid sites and lower B/L ratio than HZSM-5.

### *3.2 Catalytic dehydration of ethanol*

Aluminosilicates prepared by NHSG were tested as catalysts for the gas-phase ethanol dehydration in the temperature range between 205 and 310 °C and compared to the two benchmark catalysts – amorphous silica-alumina catalyst support (SACS) and crystalline zeolite HZSM-5. The major products of the catalytic reaction were ethylene and diethylether with carbon balances reaching 90–100 %. No other products were observed except for HZSM-5, which produced low amounts of acetaldehyde, propene, and butenes (~0.5–2 % in selectivity to these by-products in total, Table 1S).

In a first screening on the effect of temperature, we observed that the production of diethylether was favoured at lower temperatures (205–240 °C) over NHSG prepared samples and HZSM-5, while high ethylene selectivity was observed at 275 and 310 °C (Fig. 13S and Fig. 14S, Table 1S), similar to other reports on ethanol dehydration.[12,19,73] The silica alumina benchmark catalyst (SACS) showed lower activity and relatively high selectivity to ethylene was only obtained at

345 °C. This fact can be associated with the poor homogeneity of Si-Al mixing in SACS. The Lewis acid sites formed by the alumina domains are weak, leading to the necessity of applying fairly higher temperatures in order to catalyse the dehydration to ethylene.[12]

All fresh catalysts were tested again at a constant temperature of 240°C. At the beginning of the experiment, the catalytic activity of all four NHSG prepared samples was very similar (Fig. 6, Table 2S). This is in a good agreement with characterization data, which show that structure, homogeneity of Si-Al mixing, and number, strength, and nature of acid sites were similar for all NHSG prepared catalysts. The differences in textural properties described above do not seem to affect markedly the initial values of activity and selectivity. Full conversion and high selectivity was achieved with HZSM-5 at the beginning of the experiment, expectedly outperforming the NHSG catalysts. On the contrary, amorphous silica alumina was much worse than NHSG catalysts (Fig. 6, Table 2S). The marked improvement of catalytic activity in comparison to commercial silica alumina can be explained by the fact that NHSG prepared aluminosilicates exhibited acidic properties (acid sites strength and B/L ratios) intermediate between HZSM-5 and SACS. Benchmark silica alumina possesses a higher number of acid sites than NHSG prepared catalysts, but these sites are mostly weak Lewis sites which have been suggested to be poorly active in ethanol dehydration.[32] On the contrary, the high homogeneity of the aluminosilicates prepared by NHSG ensures the formation of stronger and thus more active acid sites.

### *3.3 Deactivation with time on stream*

As catalyst deactivation is a major issue for the targeted application, this test at 240°C was continued for a 15 h TOS to assess the stability of the catalysts (Fig. 6, Table 2S). On the one hand, the conversion was very stable both for the samples prepared by the acetamide elimination route and for HZSM-5. On the other hand, the conversion over catalysts prepared by the ether route and SACS decreased over time (Fig. 6 left). Ethylene selectivity tended to decrease slowly (from – 5% to –15% drop after 15 h, Table 2S) for all studied catalysts except for commercial silica alumina, where the initially very low selectivity level tended to increase over time (Fig. 6 right). The most stable NHSG catalyst was **16Si-1Al-Ac-T**, combining a very stable conversion and a very moderate

decrease in ethylene selectivity (−9%) after 15 h. It is important to note that, while HZSM-5 appears to be the catalyst with the highest performance and stability, some by-products were observed in this case (i.e. acetaldehyde, propene, and butenes, in addition to diethylether). Moreover, coke formation was suspected, based on the pale brown color of the catalyst after this experiment. The NHSG catalysts did not exhibit any change of color indicating no coke formation.

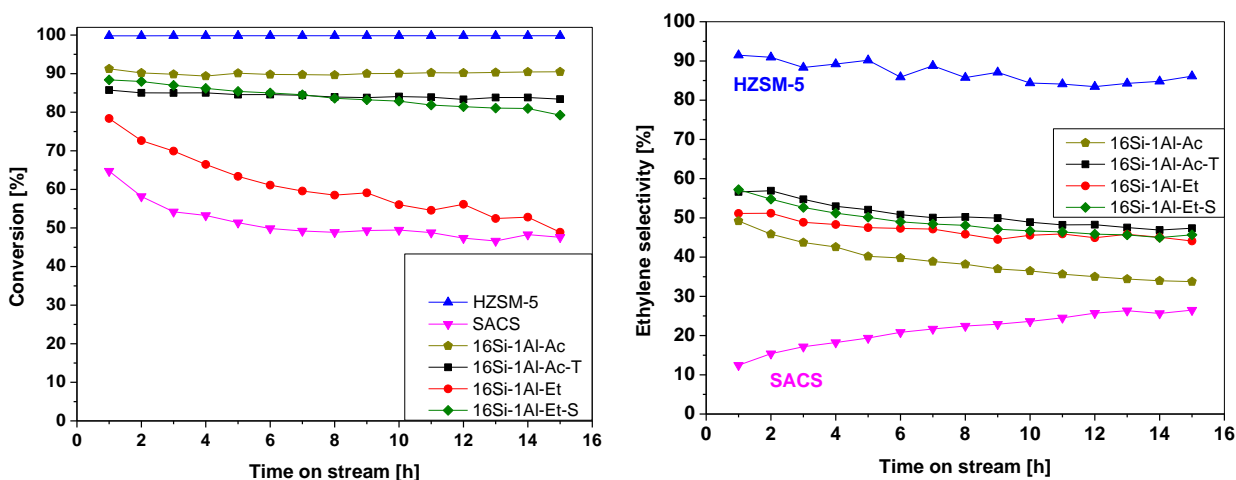


Fig. 6: Conversion (left) and ethylene selectivity (right) at 240 °C over benchmark and NHSG prepared catalysts during 15 h TOS stability test.

The textural properties were reanalysed after 15 h on stream (Table 2). An abrupt decrease of surface area and pore volume was observed for catalysts with decreasing catalytic activity with TOS: **16Si-1Al-Et** (−50 %  $SA_{BET}$  and −46 %  $V_{total}$ ), **16Si-1Al-Et-S** (−31 %  $SA_{BET}$  and −52 %  $V_{total}$ ), and commercial silica-alumina (−35 %  $SA_{BET}$  and −51 %  $V_{total}$ ). **16Si-1Al-Ac**, which displayed rather stable conversion but decreasing selectivity, also exhibited a marked decrease of surface area and pore volume (−43 %  $SA_{BET}$  and −54 %  $V_{total}$ ). While HZSM-5 is presumed to be stable after the experiment presented in Fig. 6, it displayed a strong decrease of the pore volume (−23 %, Table 3S). Finally, **16Si-1Al-Ac-T**, which was pointed as catalytically stable, was the only sample that exhibited only minor loss of surface area (−6 %) and no loss of pore volume. This finding points at the robustness of the “wormhole” texture under the reaction conditions (240 °C, ethanol and water vapor). It seems that, unlike the microporous channels of **16Si-1Al-Ac** or the nanoparticle

aggregates of **16Si-Al-Et** and **16Si-1Al-Et-S** which appear to be prone to hydrothermal ageing and pore collapse, the more open texture of **16Si-1Al-Ac-T** offers a better resistance to those deactivating phenomena. Altogether, based on its good catalytic performance and high stability with TOS, **16Si-1Al-Ac-T** was selected for further studies as the most promising sample out of NHSG aluminosilicate catalysts prepared in this study.

### *3.4 Catalyst stability at maximum productivity*

Samples **16Si-1Al-Ac-T** and HZSM-5 were chosen to further investigate stability issues. In the conditions presented above (Fig. 6), **16Si-1Al-Ac-T** exhibited a stable conversion of ~85%. The HZSM-5 zeolite on the other hand displayed full conversion over the timespan of the test. In fact, for this very active catalyst it is necessary to adapt the WHSV to ensure that the catalyst amount is not in excess with respect to the feed of reactant. To compare stability, it is important to ensure that the total mass of catalysts is employed in the catalytic reaction (otherwise, a stable performance level can be observed simply because the deactivated catalyst located at the beginning of the bed is constantly being compensated by “fresh” catalyst located further in the bed). Thus, maximum ethylene productivity was found by increasing the reactant flow (keeping concentration of ethanol constant in the feed) until the ethanol conversion dropped from 100 to ~95%. This was obtained with a N<sub>2</sub> flow of ~80 cm<sup>3</sup> min<sup>-1</sup> and ethanol feed 0.45 g h<sup>-1</sup> for 0.192 g of **16Si-1Al-Ac-T** at 275 °C and a N<sub>2</sub> flow of ~150 cm<sup>3</sup> min<sup>-1</sup> and ethanol feed 0.84 g h<sup>-1</sup> for 0.048 g of HZSM-5 at 240 °C. Different temperatures were chosen in order to have comparable ethylene selectivity for both catalysts (above 90 %). The higher catalytic activity of HZSM-5 was reflected in higher ethylene productivity in this experiment: 8.34 g<sub>ethylene</sub> g<sub>cat</sub><sup>-1</sup> h<sup>-1</sup> for HZSM-5 at 240 °C and 1.32 g<sub>ethylene</sub> g<sub>cat</sub><sup>-1</sup> h<sup>-1</sup> for **16Si-1Al-Ac-T** at 275 °C.

An important difference in stability was observed (Fig. 7, Table 4S). While the NHSG-made aluminosilicate gave stable conversion, HZSM-5 displayed a marked drop of ca. 20 % during 15 h (Fig. 7 left). Again, ethylene selectivity had a slowly decreasing trend for both catalysts (Fig. 7 right). All in all, the ethylene yield for **16Si-1Al-Ac-T** was only slightly decreasing with time (-15%) because the catalyst progressively produced more diethylether (5 % yield at the beginning and 14

% at the end of the experiment, Table 4S). This can tentatively be attributed to some *in situ* modifications of the strongest Lewis acid sites in **16Si-1Al-Ac-T**, possibly under the action of water.[65,74]

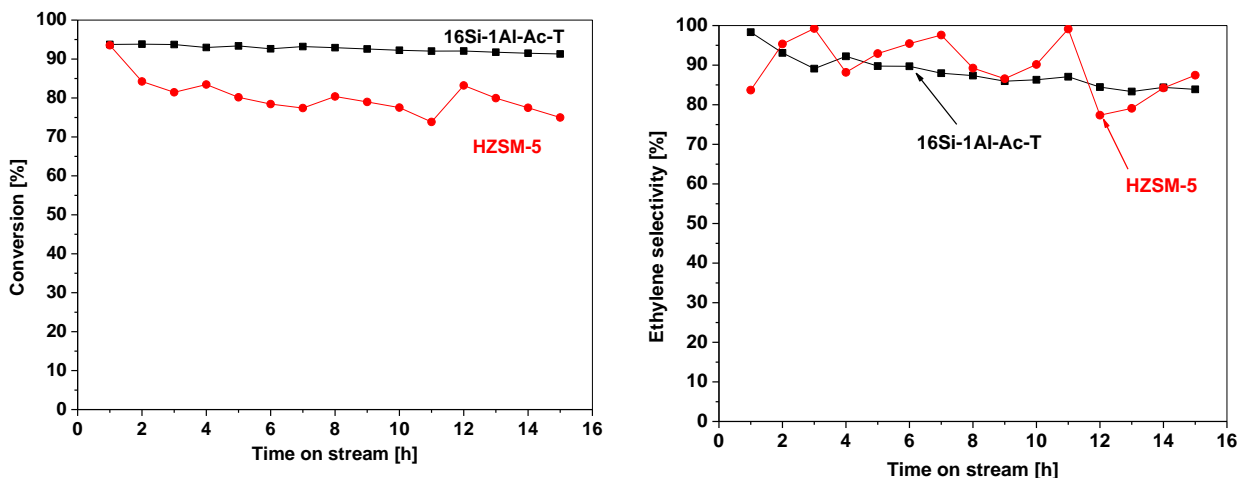


Fig. 7: Conversion (left) and ethylene yield (right) over HZSM-5 and 16Si-1Al-Ac-T at their maximum productivity during 15 h TOS stability test.

HZSM-5 deactivation was presumably caused by coke deposition due to the presence of strong Brønsted acid sites promoting ethylene oligomerization.[16,17,21,22] This suggestion can be supported by several observations: (i) HZSM-5 produced small amounts of acetaldehyde, propene, and butenes (these molecules are easily oligomerized/polymerized); (ii) fresh HZSM-5 was totally white spent HZSM-5 was pale brown; (iii) the pore volume decreased by 26 % ( $N_2$  physisorption, Table 3S); (iv) a weak band was observed in Raman spectra of spent HZSM-5 at ca.  $1400\text{ cm}^{-1}$  (Fig. 15S). This band is usually observed in Raman spectra of coked zeolites and can originate from “disordered” polyaromatic coke structures.[19] In contrary to HZSM-5 neither acetaldehyde nor butenes were observed for **16Si-1Al-Ac-T**. This catalyst also kept its pale yellow color, and both pore volume and surface area were stable ( $-6$  and  $-11$  %, respectively, Table 3S). Finally  $400\text{--}4000\text{ cm}^{-1}$  region in Raman spectra was completely clean in the case of fresh HZSM-5, and both fresh and spent **16Si-1Al-Ac-T** (Fig. 15S). Thus, the presented data suggest that, while

HZSM-5 suffered from deactivation caused by coking, the aluminosilicate catalyst prepared by NHSG displayed stable catalytic performance and no coking.

#### **4. Conclusions**

Amorphous aluminosilicate catalysts were prepared by non-hydrolytic sol-gel technique and described by a number of physico-chemical methods. Textural properties could be controlled by changing the amount of solvent used or by the application of templating agent. Samples were ranging from microporous to mesoporous with high pore volume (up to  $0.96 \text{ g cm}^{-3}$ ). Importantly, the homogeneity of Si-Al mixing was very high:  $^{27}\text{Al}$  MAS NMR spectra of dehydrated samples with adsorbed pyridine exhibited a single signal originating from tetrahedrally coordinated aluminum species, i.e. no alumina particles were formed within silica matrices. Thus, these aluminosilicates exhibited an intermediate acidity in between zeolite HZSM-5 and commercial silica alumina catalyst support in terms of acid sites strength and B/L ratio.

Aluminosilicate catalysts prepared by NHSG were tested in ethanol dehydration and showed activity significantly higher than commercial amorphous silica-alumina benchmark, thanks to the high homogeneity of Al dispersion, but lower than HZSM-5, owing to their milder acidity. As a result, neither oligomerization of ethylene nor coking was observed with NHSG materials unlike with HZSM-5. The most stable aluminosilicate catalyst was compared to HZSM-5 in a stability test at maximum productivity. While conversion was markedly decreasing with time on stream over HZSM-5, due to coking, conversion over NHSG aluminosilicate was stable during 15 h TOS. We anticipate that such aluminosilicate materials with a high degree of Si-Al mixing and open mesoporosity could represent an attractive alternative to zeolites for long term operation in (bio)ethanol dehydration.

#### **Acknowledgements**

A.S. acknowledges funding from the European Union's Horizon 2020 research and innovation programme under the Marie Skłodowska-Curie grant agreement No 751774. Authors acknowledge the 'Communauté française de Belgique' for the financial support through the ARC programme (15/20-069). François Devred and Jean-François Statsyns are acknowledged for the

technical and logistical support. This research used resources of the “Plateforme Technologique Physico-Chimique Characterization” – PC2, the SIAM platform (Synthesis, Irradiation & Analysis of Materials) and the MORPH-IM platform (Morphology & Imaging) located at the University of Namur. Authors thank L. Simonikova for performing ICP-OES analyses. CIISB research infrastructure project LM2015043 funded by MEYS CR is gratefully acknowledged for the financial support of the measurements at the CF Cryo-electron Microscopy and Tomography.

## References

- [1] M. Behrens, A.K. Datye, *Catalysis for the Conversion of Biomass and Its Derivatives*, Ed. Open Access, Berlin, 2013. <https://books.google.cz/books?id=46qHRqaQdEQC>.
- [2] J. Sun, Y. Wang, Recent advances in catalytic conversion of ethanol to chemicals, *ACS Catal.* 4 (2014) 1078–1090. <https://doi.org/10.1021/cs4011343>.
- [3] D. Cespi, F. Passarini, I. Vassura, F. Cavani, Butadiene from biomass, a life cycle perspective to address sustainability in the chemical industry, *Green Chem.* 18 (2016) 1625–1638. <https://doi.org/10.1039/C5GC02148K>.
- [4] I. Rossetti, M. Compagnoni, E. Finocchio, G. Ramis, A. Di Michele, Y. Millot, S. Dzwigaj, Ethylene production via catalytic dehydration of diluted bioethanol: A step towards an integrated biorefinery, *Appl. Catal. B Environ.* 210 (2017) 407–420. <https://doi.org/10.1016/J.APCATB.2017.04.007>.
- [5] C. Angelici, B.M. Weckhuysen, P.C.A. Bruijninx, Chemocatalytic conversion of ethanol into butadiene and other bulk chemicals, *ChemSusChem.* 6 (2013) 1595–1614. <https://doi.org/10.1002/cssc.201300214>.
- [6] M. Zhang, Y. Yu, Dehydration of ethanol to ethylene, *Ind. Eng. Chem. Res.* 52 (2013) 9505–9514. <https://doi.org/10.1021/ie401157c>.
- [7] D. Fan, D.J. Dai, H.S. Wu, Ethylene formation by catalytic dehydration of ethanol with industrial considerations, *Materials (Basel).* 6 (2013) 101–115. <https://doi.org/10.3390/ma6010101>.
- [8] G. Garbarino, R. Prasath Parameswari Vijayakumar, P. Riani, E. Finocchio, G. Busca, Ethanol and diethyl ether catalytic conversion over commercial alumina and lanthanum-doped alumina: Reaction paths, catalyst structure and coking, *Appl. Catal. B Environ.* (2018). <https://doi.org/10.1016/j.apcatb.2018.05.039>.
- [9] J.F. DeWilde, H. Chiang, D.A. Hickman, C.R. Ho, A. Bhan, Kinetics and mechanism of ethanol dehydration on  $\gamma$ -Al<sub>2</sub>O<sub>3</sub>: The critical role of dimer inhibition, *ACS Catal.* 3 (2013) 798–807. <https://doi.org/10.1021/cs400051k>.
- [10] W. Alharbi, E. Brown, E.F. Kozhevnikova, I. V. Kozhevnikov, Dehydration of ethanol over heteropoly acid catalysts in the gas phase, *J. Catal.* 319 (2014) 174–181. <https://doi.org/10.1016/j.jcat.2014.09.003>.



- [11] L. Matachowski, M. Zimowska, D. Mucha, T. Machej, Ecofriendly production of ethylene by dehydration of ethanol over Ag 3PW 12O 40 salt in nitrogen and air atmospheres, *Appl. Catal. B Environ.* (2012). <https://doi.org/10.1016/j.apcatb.2012.05.003>.
- [12] T.K. Phung, G. Busca, Ethanol dehydration on silica-aluminas: Active sites and ethylene/diethyl ether selectivities, *Catal. Commun.* 68 (2015) 110–115. <https://doi.org/10.1016/J.CATCOM.2015.05.009>.
- [13] G. Busca, Silica-alumina catalytic materials: A critical review, *Catal. Today.* (2019) 1–9. <https://doi.org/10.1016/j.cattod.2019.05.011>.
- [14] G. Chen, S. Li, F. Jiao, Q. Yuan, Catalytic dehydration of bioethanol to ethylene over TiO<sub>2</sub>/γ-Al<sub>2</sub>O<sub>3</sub> catalysts in microchannel reactors, *Catal. Today.* 125 (2007) 111–119. <https://doi.org/10.1016/j.cattod.2007.01.071>.
- [15] J. Bedia, R. Barrionuevo, J. Rodríguez-Mirasol, T. Cordero, Ethanol dehydration to ethylene on acid carbon catalysts, *Appl. Catal. B Environ.* 103 (2011) 302–310. <https://doi.org/10.1016/j.apcatb.2011.01.032>.
- [16] C.P. Nash, A. Ramanathan, D.A. Ruddy, M. Behl, E. Gjersing, M. Griffin, H. Zhu, B. Subramaniam, J.A. Schaidle, J.E. Hensley, Mixed alcohol dehydration over Brønsted and Lewis acidic catalysts, *Appl. Catal. A Gen.* 510 (2016) 110–124. <https://doi.org/10.1016/j.apcata.2015.11.019>.
- [17] X. Zhang, R. Wang, X. Yang, F. Zhang, Comparison of four catalysts in the catalytic dehydration of ethanol to ethylene, *Microporous Mesoporous Mater.* 116 (2008) 210–215. <https://doi.org/10.1016/j.micromeso.2008.04.004>.
- [18] M.E. Potter, M.E. Cholerton, J. Kezina, R. Bounds, M. Carravetta, M. Manzoli, E. Gianotti, M. Lefenfeld, R. Raja, Role of Isolated Acid Sites and Influence of Pore Diameter in the Low-Temperature Dehydration of Ethanol, *ACS Catal.* 4 (2014) 4161–4169. <https://doi.org/10.1021/cs501092b>.
- [19] T.K. Phung, L. Proietti Hernández, A. Lagazzo, G. Busca, Dehydration of ethanol over zeolites, silica alumina and alumina: Lewis acidity, Brønsted acidity and confinement effects, *Appl. Catal. A Gen.* 493 (2015) 77–89. <https://doi.org/10.1016/j.apcata.2014.12.047>.
- [20] T.M. Nguyen, R. Le Van Mao, Conversion of ethanol in aqueous solution over ZSM-5 zeolites, *Appl. Catal.* 58 (1990) 119–129. [https://doi.org/10.1016/S0166-9834\(00\)82282-4](https://doi.org/10.1016/S0166-9834(00)82282-4).

- [21] C.B. Phillips, R. Datta, Production of Ethylene from Hydrous Ethanol on H-ZSM-5 under Mild Conditions, *Ind. Eng. Chem. Res.* 36 (1997) 4466–4475. <https://doi.org/10.1021/ie9702542>.
- [22] J. Bi, X. Guo, M. Liu, X. Wang, High effective dehydration of bio-ethanol into ethylene over nanoscale HZSM-5 zeolite catalysts, *Catal. Today.* 149 (2010) 143–147. <https://doi.org/10.1016/j.cattod.2009.04.016>.
- [23] B. Chen, J. Lu, L. Wu, Z. Chao, Dehydration of bio-ethanol to ethylene over iron exchanged HZSM-5, *Chinese J. Catal.* 37 (2016) 1941–1948. [https://doi.org/10.1016/S1872-2067\(16\)62524-X](https://doi.org/10.1016/S1872-2067(16)62524-X).
- [24] K. Ramesh, L.M. Hui, Y.F. Han, A. Borgna, Structure and reactivity of phosphorous modified H-ZSM-5 catalysts for ethanol dehydration, *Catal. Commun.* 10 (2009) 567–571. <https://doi.org/10.1016/j.catcom.2008.10.034>.
- [25] H. Xin, X. Li, Y. Fang, X. Yi, W. Hu, Y. Chu, F. Zhang, A. Zheng, H. Zhang, X. Li, Catalytic dehydration of ethanol over post-treated ZSM-5 zeolites, *J. Catal.* 312 (2014) 204–215. <https://doi.org/10.1016/j.jcat.2014.02.003>.
- [26] J.M. Müller, G.C. Mesquita, S.M. Franco, L.D. Borges, J.L. de Macedo, J.A. Dias, S.C.L. Dias, Solid-state dealumination of zeolites for use as catalysts in alcohol dehydration, *Microporous Mesoporous Mater.* 204 (2015) 50–57. <https://doi.org/10.1016/J.MICROMESO.2014.11.002>.
- [27] M. Krossner, J. Sauer, Interaction of Water with Brønsted Acidic Sites of Zeolite Catalysts. Ab Initio Study of 1:1 and 2:1 Surface Complexes, *J. Phys. Chem.* 100 (1996) 6199–6211. <https://doi.org/10.1021/jp952775d>.
- [28] Q. Sheng, S. Guo, K. Ling, L. Zhao, Catalytic dehydration of ethanol to ethylene over alkali-treated HZSM-5 zeolites, *J. Braz. Chem. Soc.* 25 (2014) 1365–1371. <https://doi.org/10.5935/0103-5053.20140118>.
- [29] Q. Sheng, K. Ling, Z. Li, L. Zhao, Effect of steam treatment on catalytic performance of HZSM-5 catalyst for ethanol dehydration to ethylene, *Fuel Process. Technol.* 110 (2013) 73–78. <https://doi.org/10.1016/j.fuproc.2012.11.004>.
- [30] K.K. Ramasamy, H. Zhang, J. Sun, Y. Wang, Conversion of ethanol to hydrocarbons on hierarchical HZSM-5 zeolites, *Catal. Today.* 238 (2014) 103–110. <https://doi.org/10.1016/j.cattod.2014.01.037>.
- [31] T.K. Phung, A. Lagazzo, M.Á. Rivero Crespo, V. Sánchez Escribano, G. Busca, A study of commercial

- transition aluminas and of their catalytic activity in the dehydration of ethanol, *J. Catal.* 311 (2014) 102–113. <https://doi.org/10.1016/j.jcat.2013.11.010>.
- [32] M. Caillot, A. Chaumonnot, M. Digne, J.A. Vanbokhoven, Creation of Brønsted acidity by grafting aluminum isopropoxide on silica under controlled conditions: Determination of the number of Brønsted Sites and their turnover frequency for *m*-xylene isomerization, *ChemCatChem*. 6 (2014) 832–841. <https://doi.org/10.1002/cctc.201300824>.
- [33] M. Caillot, A. Chaumonnot, M. Digne, J.A. Van Bokhoven, The variety of Brønsted acid sites in amorphous aluminosilicates and zeolites, *J. Catal.* 316 (2014) 47–56. <https://doi.org/10.1016/j.jcat.2014.05.002>.
- [34] J.H. Kwak, D. Mei, C.H.F. Peden, R. Rousseau, J. Szanyi, (100) facets of  $\gamma$ -Al<sub>2</sub>O<sub>3</sub>: The active surfaces for alcohol dehydration reactions, *Catal. Letters*. 141 (2011) 649–655. <https://doi.org/10.1007/s10562-010-0496-8>.
- [35] M. Caillot, A. Chaumonnot, M. Digne, J.A. Van Bokhoven, Quantification of Brønsted Acid Sites of Grafted Amorphous Silica-Alumina Compounds and their Turnover Frequency in *m*-Xylene Isomerization, *ChemCatChem*. 5 (2013) 3644–3656. <https://doi.org/10.1002/cctc.201300560>.
- [36] M. Caillot, A. Chaumonnot, M. Digne, C. Poleunis, D.P. Debecker, J.A. van Bokhoven, Synthesis of amorphous aluminosilicates by grafting: Tuning the building and final structure of the deposit by selecting the appropriate synthesis conditions, *Microporous Mesoporous Mater.* 185 (2014) 179–189. <https://doi.org/10.1016/j.micromeso.2013.10.032>.
- [37] D.P. Debecker, C. Boissière, G. Laurent, S. Huet, P. Eliaers, C. Sanchez, R. Backov, B. Bujoli, Z. Gan, G. Hoatson, First acidic macro-mesocellular aluminosilicate monolithic foams “SiAl(HIPE)” and their catalytic properties, *Chem. Commun.* 51 (2015) 14018–14021. <https://doi.org/10.1039/C5CC05328E>.
- [38] A. Styskalik, D. Skoda, C.E. Barnes, J. Pinkas, The Power of Non-Hydrolytic Sol-Gel Chemistry: A Review, *Catalysts*. 7 (2017) 168. <https://doi.org/10.3390/catal7060168>.
- [39] D.P. Debecker, P.H. Mutin, Non-hydrolytic sol–gel routes to heterogeneous catalysts, *Chem. Soc. Rev.* 41 (2012) 3624–3650. <https://doi.org/10.1039/C2CS15330K>.
- [40] D. Skoda, A. Styskalik, Z. Moravec, P. Bezdicka, M. Babiak, M. Klementova, C.E. Barnes, J. Pinkas, Novel non-hydrolytic templated sol–gel synthesis of mesoporous aluminosilicates and their use as

- aminolysis catalysts, *RSC Adv.* 6 (2016) 24273–24284. <https://doi.org/10.1039/C5RA24563J>.
- [41] S. Acosta, R. Corriu, D. Leclercq, P.H. Mutin, A. Vioux, Novel Non-Hydrolytic Sol-Gel Route to Metal Oxides, *J. Sol-Gel Sci. Technol.* 2 (1994) 25–28. <https://doi.org/10.1007/BF00486208>.
- [42] D.D. Dochain, A. Stýskalík, D.P. Debecker, Ag- and Cu-Promoted Mesoporous Ta-SiO<sub>2</sub> Catalysts Prepared by Non-Hydrolytic Sol-Gel for the Conversion of Ethanol to Butadiene, *Catalysts.* 9 (2019) 920. <https://doi.org/10.3390/catal9110920>.
- [43] B.L. Caetano, L.A. Rocha, E. Molina, Z.N. Rocha, G. Ricci, P.S. Calefi, O.J. de Lima, C. Mello, E.J. Nassar, K.J. Ciuffi, Cobalt aluminum silicate complexes prepared by the non-hydrolytic sol-gel route and their catalytic activity in hydrocarbon oxidation, *Appl. Catal. A Gen.* 311 (2006) 122–134. <https://doi.org/10.1016/j.apcata.2006.06.028>.
- [44] D.P. Debecker, K. Bouchmella, C. Poleunis, P. Eloy, P. Bertrand, E.M. Gaigneaux, P.H. Mutin, Design of SiO<sub>2</sub>-Al<sub>2</sub>O<sub>3</sub>-MoO<sub>3</sub> Metathesis Catalysts by Nonhydrolytic Sol-Gel, *Chem. Mater.* 21 (2009) 2817–2824. <https://doi.org/10.1021/cm900490t>.
- [45] K. Bouchmella, M. Stoyanova, U. Rodemerck, D.P. Debecker, P. Hubert Mutin, Avoiding rhenium loss in non-hydrolytic synthesis of highly active Re-Si-Al olefin metathesis catalysts, *Catal. Commun.* 58 (2015) 183–186. <https://doi.org/10.1016/j.catcom.2014.09.024>.
- [46] D.P. Debecker, Innovative Sol-Gel Routes for the Bottom-Up Preparation of Heterogeneous Catalysts, *Chem. Rec.* 18 (2018) 662–675. <https://doi.org/10.1002/tcr.201700068>.
- [47] D.P. Debecker, V. Hulea, P.H. Mutin, Mesoporous mixed oxide catalysts via non-hydrolytic sol-gel: A review, *Appl. Catal., A.* 451 (2013) 192–206. <https://doi.org/10.1016/j.apcata.2012.11.002>.
- [48] V. Lafond, P.H. Mutin, A. Vioux, Control of the Texture of Titania-Silica Mixed Oxides Prepared by Nonhydrolytic Sol-Gel, *Chem. Mater.* 16 (2004) 5380–5386. <https://doi.org/10.1021/cm0490569>.
- [49] A. Styskalik, D. Skoda, J. Pinkas, S. Mathur, Non-hydrolytic synthesis of titanosilicate xerogels by acetamide elimination and their use as epoxidation catalysts, *J. Sol-Gel Sci. Technol.* 63 (2012) 463–472. <https://doi.org/10.1007/s10971-012-2808-5>.
- [50] D. Skoda, A. Styskalik, Z. Moravec, P. Bezdicka, C.E.C.E. Barnes, J. Pinkas, Mesoporous titanosilicates by templated non-hydrolytic sol-gel reactions, *J. Sol-Gel Sci. Technol.* 74 (2015) 810–822. <https://doi.org/10.1007/s10971-015-3666-8>.
- [51] A. Styskalik, I. Kordoghli, C. Poleunis, A. Delcorte, C. Aprile, L. Fusaro, D. Debecker, Highly Porous

Hybrid Metallosilicate Materials Prepared by Non-Hydrolytic Sol-Gel: Hydrothermal Stability and Catalytic Properties in Ethanol Dehydration, (2019).

<https://doi.org/10.26434/CHEMRXIV.9114413.V1>.

- [52] J.W. Kriesel, M.S. Sander, T.D. Tilley, Block Copolymer-Assisted Synthesis of Mesoporous, Multicomponent Oxides by Nonhydrolytic, Thermolytic Decomposition of Molecular Precursors in Nonpolar Media, *Chem. Mater.* 13 (2001) 3554–3563. <https://doi.org/10.1021/cm010068t>.
- [53] N. Godard, A. Vivian, L. Fusaro, L. Cannavici, C. Aprile, D.P. Debecker, High-Yield Synthesis of Ethyl Lactate with Mesoporous Tin Silicate Catalysts Prepared by an Aerosol-Assisted Sol-Gel Process, *ChemCatChem*. 9 (2017) 2211–2218. <https://doi.org/10.1002/cctc.201601637>.
- [54] D. Skoda, A. Styskalik, Z. Moravec, P. Bezdicka, J. Pinkas, Templated non-hydrolytic synthesis of mesoporous zirconium silicates and their catalytic properties, *J. Mater. Sci.* 50 (2015) 3371–3382. <https://doi.org/10.1007/s10853-015-8888-1>.
- [55] Y. Hirata, K. Sakeda, Y. Matsushita, K. Shimada, Y. Ishihara, Characterization and Sintering Behavior of Alkoxide-Derived Aluminosilicate Powders, *J. Am. Ceram. Soc.* 72 (1989) 995–1002. <https://doi.org/10.1111/j.1151-2916.1989.tb06258.x>.
- [56] E. Ruiz de Sola, F. Estevan, F.J. Torres, J. Alarcón, Effect of thermal treatment on the structural evolution of 3:2 and 2:1 mullite monophasic gels, *J. Non. Cryst. Solids*. 351 (2005) 1202–1209. <https://doi.org/10.1016/j.jnoncrysol.2005.02.017>.
- [57] C.S. Blackwell, Investigation of zeolite frameworks by vibrational properties. 1. The double-four-ring in group 3 zeolites, *J. Phys. Chem.* 83 (1979) 3251–3257. <https://doi.org/10.1021/j100488a014>.
- [58] M. Toba, F. Mizukami, S. Niwa, T. Sano, K. Maeda, H. Shoji, Effect of preparation methods on properties of amorphous alumina/silicas, *J. Mater. Chem.* 4 (1994) 1131–1135.
- [59] A. Styskalik, J.G. Abbott, M.C. Orick, D.P. Debecker, C.E. Barnes, Synthesis, characterization and catalytic activity of single site, Lewis acidic aluminosilicates, *Catal. Today*. (2018) 1–9. <https://doi.org/10.1016/j.cattod.2018.11.079>.
- [60] J.A. Van Bokhoven, A.M.J. Van der Eerden, D.C. Koningsberger, Three-coordinate aluminum in zeolites observed with in situ x-ray absorption near-edge spectroscopy at the Al K-edge: Flexibility of aluminum coordinations in zeolites, *J. Am. Chem. Soc.* 125 (2003) 7435–7442.

<https://doi.org/10.1021/ja0292905>.

- [61] Z. Wang, Y. Jiang, O. Lafon, J. Trébosc, K. Duk Kim, C. Stampfl, A. Baiker, J.-P. Amoureux, J. Huang, Brønsted acid sites based on penta-coordinated aluminum species, *Nat. Commun.* 7 (2016) 13820. <https://doi.org/10.1038/ncomms13820>.
- [62] Z. Wang, Y. Jiang, X. Yi, C. Zhou, A. Rawal, J. Hook, Z. Liu, F. Deng, A. Zheng, M. Hunger, A. Baiker, J. Huang, High population and dispersion of pentacoordinated Al V species on the surface of flame-made amorphous silica-alumina, *Sci. Bull.* 64 (2019) 516–523. <https://doi.org/10.1016/j.scib.2019.04.002>.
- [63] Z. Wang, Y. Jiang, F. Jin, C. Stampfl, M. Hunger, A. Baiker, J. Huang, Strongly enhanced acidity and activity of amorphous silica–alumina by formation of pentacoordinated Al V species, *J. Catal.* 372 (2019) 1–7. <https://doi.org/10.1016/j.jcat.2019.02.007>.
- [64] S. Pega, C. Boissière, D. Grosso, T. Azaïs, A. Chaumonnot, C. Sanchez, Direct Aerosol Synthesis of Large-Pore Amorphous Mesoporous Aluminosilicates with Superior Acid-Catalytic Properties, *Angew. Chemie Int. Ed.* 48 (2009) 2784–2787. <https://doi.org/10.1002/anie.200805217>.
- [65] Z. Wang, L.A. O'Dell, X. Zeng, C. Liu, S. Zhao, W. Zhang, M. Gaborieau, Y. Jiang, J. Huang, Insight into Three-Coordinate Aluminum Species on Ethanol-to-Olefin Conversion over ZSM-5 Zeolites, *Angew. Chemie Int. Ed.* 58 (2019) 18061–18068. <https://doi.org/10.1002/anie.201910987>.
- [66] D.P. Debecker, M. Stoyanova, U. Rodemerck, P. Eloy, A. Léonard, B.-L. Su, E.M. Gaigneaux, Thermal Spreading As an Alternative for the Wet Impregnation Method: Advantages and Downsides in the Preparation of  $\text{MoO}_3/\text{SiO}_2-\text{Al}_2\text{O}_3$  Metathesis Catalysts, *J. Phys. Chem. C.* 114 (2010) 18664–18673. <https://doi.org/10.1021/jp1074994>.
- [67] Emeis C. A., Determination of integrated molar extinction coefficients for Infrared absorption Bands of Pyridine Adsorbed on Solid Acid Catalysts, *J. Catal.* 141 (1993) 347–354.
- [68] M. Trombetta, G. Busca, S. Rossini, V. Piccoli, U. Cornaro, A. Guercio, R. Catani, R.J. Willey, FT-IR Studies on Light Olefin Skeletal Isomerization Catalysis, *J. Catal.* 179 (1998) 581–596. <https://doi.org/10.1006/jcat.1998.2251>.
- [69] E.J.M. Hensen, D.G. Poduval, V. Degirmenci, D.A.J.M. Ligthart, W. Chen, F. Maugé, M.S. Rigutto, J.A.R. Van Veen, Acidity characterization of amorphous silica-alumina, *J. Phys. Chem. C.* 116 (2012) 21416–21429. <https://doi.org/10.1021/jp309182f>.

- [70] E.J.M. Hensen, D.G. Poduval, D.A.J.M. Ligthart, J.A.R. Van Veen, M.S. Rigutto, Quantification of strong brønsted acid sites in aluminosilicates, *J. Phys. Chem. C*. 114 (2010) 8363–8374. <https://doi.org/10.1021/jp9106348>.
- [71] A. Corma, Inorganic Solid Acids and Their Use in Acid-Catalyzed Hydrocarbon Reactions, *Chem. Rev.* 95 (1995) 559–614. <https://doi.org/10.1021/cr00035a006>.
- [72] F. Leydier, C. Chizallet, A. Chaumonnot, M. Digne, E. Soyer, A.A. Quoineaud, D. Costa, P. Raybaud, Brønsted acidity of amorphous silica-alumina: The molecular rules of proton transfer, *J. Catal.* 284 (2011) 215–229. <https://doi.org/10.1016/j.jcat.2011.08.015>.
- [73] T.K. Phung, G. Busca, Diethyl ether cracking and ethanol dehydration: Acid catalysis and reaction paths, *Chem. Eng. J.* 272 (2015) 92–101. <https://doi.org/10.1016/j.cej.2015.03.008>.
- [74] J. Blanchard, J.M. Krafft, C. Dupont, C. Sayag, T. Takahashi, H. Yasuda, On the influence of water traces on the acidity measurement of amorphous aluminosilicates, *Catal. Today*. 226 (2014) 89–96. <https://doi.org/10.1016/j.cattod.2013.10.054>.